Influence of Semicrystalline Morphology on the Physical Aging Characteristics of Poly(phenylene sulfide)

Rajendra K. Krishnaswamy,* Jon F. Geibel, and Barbara J. Lewis

Chevron Phillips Chemical Company, LP, Bartlesville Technology Center, Bartlesville, Oklahoma 74004

Received October 25, 2002; Revised Manuscript Received February 4, 2003

ABSTRACT: We report on the influence of semicrystalline morphology on the physical aging characteristics of poly(phenylene sulfide) or PPS. Specifically, the semicrystalline morphology of PPS was described in terms of a three-phase system comprising a crystalline phase, a mobile-amorphous phase, and a rigid-amorphous phase. The physical aging kinetics were observed to depend on the relative amounts of the mobile-amorphous and rigid-amorphous phases, with accelerated aging rates measured in specimens with higher rigid-amorphous phase fraction. We suggest that the rigid-amorphous phase, which includes chain segments that are more tightly packed relative to the mobile-amorphous phase, is able to accelerate physical aging due to its relative proximity to a state of lower configurational entropy. It is also possible for localized cooperative relaxations within the rigid-amorphous phase to facilitate molecular rearrangements that accelerate the aging process. We also suggest that the configurational entropic state of the mobile- and the rigid-amorphous phases are perhaps more relevant to physical aging in semicrystalline polymers than the proximity of the aging temperature to the glass transition temperatures of the respective phases.

Background

Poly(phenylene sulfide) [PPS; poly(thio-1,4-phenylene)] is a high-performance semicrystalline thermoplastic with excellent thermal and chemical resistance properties.[1−4] PPS, in filled and neat forms, is currently utilized in a variety of market segments that include electrical, electronic, automotive, appliance, industrial, and chemical sectors. The semirigid backbone of PPS renders the crystallization kinetics to be slow enough such that an isotropic melt can be quenched to a wholly amorphous form. Crystallization is accomplished by heating the quenched amorphous polymer to temperatures above its T_g (cold-crystallization) or by slow cooling from the melt (melt-crystallization). The crystallization and melting behavior of PPS has been well studied and documented.[4−17] Crystallinity in semirigid backbone polymers such as PPS and poly(ether ether ketone) [PEEK] restricts the mobility of the noncrystalline chain segments such that the T_g of the semicrystalline polymer is substantially higher than that of the wholly amorphous counterpart. Further, calorimetric and dynamic relaxation experiments on semicrystalline PPS[9,13,16,17] and PEEK[18−22] have indicated the presence of a portion of the noncrystalline chain segments that remains rigid across the nominal glass−rubber transition of the polymer. Thus, the morphology of such semicrystalline polymers has usually been described in terms of a three-phase model that comprises a mobile-amorphous phase, a rigid-amorphous phase, and a crystalline phase.

When glasses are cooled below their glass transition temperature, they do not attain thermodynamic equilibrium due to kinetic constraints. Glassy polymers, after being cooled to below their T_g, attempt to attain equilibrium through structural rearrangements made possible through localized molecular relaxations. Such a process is referred to as physical aging. Physical aging in wholly amorphous polymers is known to influence performance properties such as mechanical integrity (modulus, impact, etc.), barrier resistance, optical properties, and so on.[23−26] Physical aging can have a particularly profound impact on polymeric products that are designed to perform for a long period of time as these materials will evolve toward equilibrium during their service life, the rate of which will depend on the proximity of the end-use temperature to the T_g of the material. While several reports document the physical aging characteristics in wholly amorphous polymers, little attention has been paid to this phenomenon in semicrystalline polymers.[27−34]

Tant and Wilkes[27] report a linear decrease in the aging rates with increasing crystallinity for PET. Their data appear to indicate that aging in semicrystalline polymers is largely a function of the crystalline weight fraction, while other reports[28,32] suggest that semicrystalline morphology could play a role in the aging process. Struik[28−31] has shown that physical aging can continue to occur at temperatures above the nominally measured T_g for semicrystalline polymers. He argues that the mobility of the noncrystalline chain segments will depend on their proximity to the lamellar crystals, with increasing mobility at locations farther away from the crystal−amorphous interface. This is not unlike the "rigid-amorphous phase" concept introduced by Wunderlich and co-workers,[18,35,36] who argue that this new phase will remain immobile as the material is heated to its T_g; this measured T_g is believed to correspond to the "mobile-amorphous phase", which is the portion of the noncrystalline phase that mobilizes at this temperature. It is further believed that the rigid-amorphous phase will mobilize over a broad temperature range extending to temperatures well above the nominally measured T_g.

Struik[28] introduced a model wherein, for the sake of simplicity, he described the glass−rubber transition of semicrystalline polymers in terms of two distinct T_gs:

* Corresponding author: e-mail krishrk@cpchem.com.

10.1021/ma025776u CCC: $25.00
Published on Web 03/28/2003

a lower T_g^L corresponding to the mobile-amorphous phase and a higher T_g^U corresponding to the rigid-amorphous phase. In this model for aging in semicrystalline polymers, Struik defines four characteristic regions as follows: region 1, $T < T_g^L$; region 2, $T \approx T_g^L$; region 3, $T_g^L < T < T_g^U$; region 4, $T \gg T_g^U$. Aging in region 1 is believed to be similar to that of an amorphous polymer. In region 1, the aging process is driven largely by the mobile-amorphous phase due to the relative proximity of the aging temperature to T_g^L. Aging in region 2 is believed to be similar to that of region 1, except that time-aging time superposition of creep data is possible only through both horizontal and downward vertical shifts. In region 3, the aging process is primarily driven by densification of the rigid-amorphous phase, which renders time aging time superposition of creep data possible through horizontal and upward vertical shifting. Aging effects are absent in region 4 as all of the noncrystalline chain segments are rubbery and in equilibrium. Secondary crystallization effects can contribute to the observed densification in region 3 and region 4; this complicates characterization of physical aging across this temperature range.

Semicrystalline PPS is increasingly finding itself in applications that require prolonged exposure to above-ambient temperatures. Consequently, physical aging of the noncrystalline phase can exert a significant influence on the long-term mechanical properties of such PPS parts. Therefore, our primary objective in this research effort is to characterize the extent and significance of physical aging in semicrystalline PPS. Further, we also wish to explore the influence exerted by the semicrystalline morphology on the physical aging characteristics in PPS.

Experimental Section

The PPS sample used in this work has a M_w of 56 281 g/mol with a $M_w/M_n = 3.0$ ($M_z = 92\,182$ g/mol). Specimens for the physical aging experiments were prepared using the following procedure. The polymer powder was melted at 320 °C for 5 min in a rectangular mold (lined with Kapton polyimide film on the outside) using a Carver compression molder. The molten PPS contained in the mold was then quenched into an ice water bath; this quenched sample was determined to be wholly amorphous (no detectable crystallinity). To generate samples of varying morphology, wholly amorphous PPS specimens were subsequently crystallized at 125, 160, and 195 °C for 4 h; this was achieved by annealing in a compression molder at the appropriate temperature. Further, a melt-crystallized specimen was also prepared by cooling the isotropic melt slowly in the compression molder after complete melting at 320 °C for 5 min. The wholly amorphous and the four semicrystalline PPS specimens were subsequently aged at ($T_{g-onset} - 15$) °C for a period of 5, 24, and 168 h.

All of the calorimetric experiments were carried out in a Perkin-Elmer DSC 7 instrument. The transition temperatures and enthalpies were calibrated using indium and zinc standards. All scans were performed from 0 to 320 °C at 20 °C/min with nitrogen blanketing the sample and reference chambers. Sample weights of approximately 6−8 mg were employed. All of the samples were analyzed at least in triplicate, and standard deviations are reported for all measured entities.

Results

Semicrystalline Morphology. Representative calorimetric traces covering the regions of the glass−rubber transition and melting for the semicrystalline samples (except the melt-crystallized sample) considered here are shown in Figure 1. These scans display two distinct melting endotherms. The peak temperature of the low-temperature endotherm (T_{m-1}) increases with increasing crystallization temperature, while the position of the high-temperature endotherm (T_{m-2}) remains largely unchanged. In fact, T_{m-1} appears to be approximately 20−30 °C above the crystallization temperature. It is generally accepted that the low-temperature endotherm is attributable to the melting of thinner, less-perfect lamellae and is a reflection of the crystallization temperature.[9] On the other hand, the high-temperature endotherm corresponds to the melting of the more dominant lamellae formed during the initial stages of the crystallization process, and its position is not as dependent on the crystallization temperature.[9] However, it is important to note that T_{m-2} is influenced by the partial melting and subsequent reorganization of the crystals during the DSC scan itself; this effect is perhaps more dominant for the cold-crystallized specimens considered here (relative to melt-crystallized specimens). The melting transition temperatures and enthalpies of the semicrystalline PPS specimens are listed in Table 1. While the enthalpy of fusion for the samples cold-crystallized at 125 and 160 °C is similar, the specimen cold-crystallized at 195 °C reveals a slightly higher heat of fusion. The melt-crystallized sample, however, displays the highest heat of fusion and also the highest peak melting temperature.

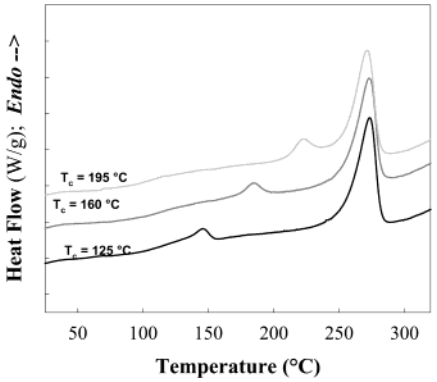

Figure 1. Representative DSC traces (20 °C/min) of the three cold-crystallized PPS samples investigated in this study.

Table 1. DSC Melting Characteristics of Wholly Amorphous and Semicrystalline PPS Specimens Used in This Study[a]

sample ID	T_{m-1} (°C)	T_{m-2} (°C)	$(\Delta H)_m$ (J/g)
PPS crystallized at 125 °C	145.0 ± 0.6	273.3 ± 0.3	38.3 ± 2.7
PPS crystallized at 160 °C	184.4 ± 0.6	272.8 ± 0.5	37.9 ± 2.5
PPS crystallized at 195 °C	224.0 ± 0.5	271.4 ± 0.1	42.3 ± 2.1
melt-crystallized PPS		282.5 ± 0.6	53.1 ± 2.1

[a] Standard deviations are based on six measurements on each sample.

The PPS samples quenched from the melt were determined to be completely amorphous; this was based on calorimetric scans, wide-angle X-ray diffraction, and density measurements. The glass transition characteristics of the amorphous and semicrystalline samples are summarized in Table 2. The reported T_g corresponds to the onset of the step change in heat capacity across the glass−rubber transition of the polymer. The T_g for the wholly amorphous PPS reported here is slightly higher than those reported previously;[9,13,16] this is due to the substantially higher molecular weight of the polymer employed in this study compared to those investigated

Table 2. Glass Transition Characteristics of Wholly Amorphous and Semicrystalline PPS Specimens Used in This Study[a]

sample ID	T_g onset (°C)	ΔC_p (T_g) (J/(g °C))
amorphous PPS	90.6 ± 0.7	0.221 ± 0.021
PPS crystallized at 125 °C	100.3 ± 0.4	0.047 ± 0.010
PPS crystallized at 160 °C	101.0 ± 2.5	0.062 ± 0.014
PPS crystallized at 195 °C	96.1 ± 0.5	0.077 ± 0.015
melt-crystallized PPS	94.3 ± 1.1	0.096 ± 0.009

[a] Standard deviations are based on six measurements on each sample.

and reported on previously. From Table 2, we note that the T_g of the semicrystalline specimens is substantially higher than that of the wholly amorphous sample. This increase in T_g is well documented and is noted to be a consequence of the constraints imposed by the crystalline lamellae on the mobility of the noncrystalline chain segments. Further, we also note a lowering of the T_g for specimens crystallized under conditions of high segmental mobility (fewer constraints), such as cold-crystallization at high temperatures and crystallization via slow cooling from the melt.

The glass−rubber transition of the PPS samples was also characterized in terms of the increment in heat capacity across the transition, or $\Delta C_p(T_g)$. For wholly amorphous PPS, the magnitude of the glass−rubber transition as characterized by ΔC_p is noted to be 0.221 J/(g °C); this value compares well with those reported in the literature.[9,13,16] The magnitude of the step change in heat capacity across the glass transition for semicrystalline polymers is a good indicator of the relative population of noncrystalline chain segments that participate in the transition. The $\Delta C_p(T_g)$ for all the semicrystalline specimens is listed in Table 2. It is important to note that the standard deviations from at least six measurements on each semicrystalline sample are approximately 15−20% of the reported averages. We note that $\Delta C_p(T_g)$ decreases with increasing crystallization temperature. This behavior is also consistent with previous reports on PPS[9,13,16] and PEEK.[18−22] At higher crystallization temperatures, segmental mobility is high such that the crystallization process experiences relatively fewer constraints; this translates to lower degrees of constraint imposed by the crystalline lamellae on the mobility of the noncrystalline chain segments in the semicrystalline polymer. As a result, a greater portion of the noncrystalline phase is able to mobilize during the observed glass transition.

The $\Delta C_p(T_g)$ values for all the semicrystalline PPS specimens, when compared to their wholly amorphous counterpart, are too small to be accounted for by the degree of crystallinity. In other words, only a fraction of the noncrystalline chain segments actually participate in the glass−rubber transition. This was recognized early by Wunderlich and co-workers,[18,35,36] and the concept of the rigid-amorphous phase was introduced to explain this discrepancy in semicrystalline polymers. Subsequently, investigators have treated the semicrystalline morphology of semirigid backbone polymers in terms of a three-phase model. The three phases include the mobile-amorphous phase, the rigid-amorphous phase, and the crystalline phase. The crystalline phase fraction (W_C) is calculated from the melting enthalpy using 114 J/g as the heat of fusion for 100% crystalline PPS.[13] The mobile-amorphous phase fraction (W_{MA}) is calculated using the formula

Table 3. Amorphous and Semicrystalline PPS Specimens Described in Terms of the Three-Phase Model Involving a Crystalline Phase, a Mobile-Amorphous Phase, and a Rigid-Amorphous Phase[a]

sample ID	W_C	W_{MA}	W_{RA}
amorphous PPS	0.00	1.00	0.00
PPS crystallized at 125 °C	0.34	0.21	0.45
PPS crystallized at 160 °C	0.33	0.28	0.39
PPS crystallized at 195 °C	0.37	0.35	0.28
melt-crystallized PPS	0.47	0.43	0.10

[a] W_C, W_{MA}, and W_{RA} are the weight fractions of the crystalline, mobile-amorphous phase, and rigid-amorphous phase, respectively.

$$W_{MA} = \frac{[\Delta C_p(T_g)]^{SC}}{[\Delta C_p(T_g)]^{AM}} \quad (1)$$

where the superscripts "SC" and "AM" correspond to semicrystalline and wholly amorphous specimens, respectively. Then, the rigid-amorphous phase fraction (W_{RA}) is calculated from a mass balance of the three phases:

$$W_{RA} = 1 - W_{MA} - W_C \quad (2)$$

The fractions of the three phases in the semicrystalline PPS specimens considered in this study are listed in Table 3. While W_C for the cold-crystallized specimens is not very different, W_{MA} is noted to increase with crystallization temperature; this is essentially a reflection of the previously discussed $\Delta C_p(T_g)$ trends with crystallization temperature. As a result, the rigid-amorphous phase fraction is observed to decrease with increasing crystallization temperature; this trend is consistent with those noted previously.[9,13,16−22] From Table 3, we also note that the melt-crystallized PPS displays the lowest rigid-amorphous phase fraction coupled with the highest crystalline weight fraction.

In general, our observations concerning the influence of thermal history on the relative proportion of the three phases in PPS are consistent with those reported previously. Specifically, when the lamellar crystals are formed under conditions of low segmental mobility, the long period (and amorphous interlayer thickness) is small; this translates to a higher degree of constraint imposed by the lamellae on the mobility of the interlamellar noncrystalline chain segments, consistent with a higher rigid-amorphous phase fraction. While the rigid-amorphous phase is noted to remain immobile across the observed glass transition, dynamic relaxation experiments suggest gradual mobilization of this phase at temperatures between the T_g and T_m of semicrystalline polymers.[17,19−22] In other words, the glass−rubber transition of the rigid-amorphous phase is thought to be very broad and occurs at temperatures above the T_g of the mobile-amorphous phase.

There is considerable debate regarding the location of the rigid-amorphous phase. Some believe that this highly constrained phase is a manifestation of gradual dissipation of the crystalline order from the lamellar surface to the bulk interlamellar regions; this means that the rigid-amorphous phase is confined to a few nanometers close to the lamellar surface within the interlamellar regions.[37,38] Others suggest that practically all of the interlamellar noncrystalline regions constitute the rigid-amorphous phase, while the mobile-amorphous phase is located largely in the interfibrillar regions of crystalline superstructures.[39,40] Our research

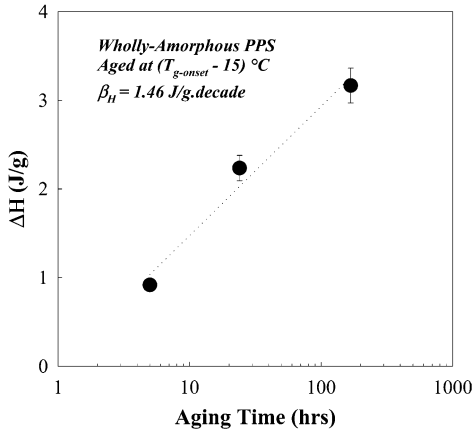

Figure 2. Recovered enthalpy (ΔH) plotted as a function of aging time for wholly amorphous PPS aged at [$T_{g-onset}$ − 15] °C.

efforts do not attempt to distinguish between the above-mentioned origins of the rigid-amorphous phase. Much of our subsequent attention will focus on the influence exerted by this phase on the physical aging characteristics of semicrystalline PPS.

Physical Aging Characteristics. The nonequilibrium glassy state of a polymer tends to proceed toward thermodynamic equilibrium through structural relaxations made possible by localized molecular or segmental motions in the glassy state. This time-dependent process of physical aging results in systematic decreases in free volume, enthalpy, and configurational entropy. This change in the thermodynamic state of the polymer can be characterized using dilatometry,[41] which measures volume changes and refractometry,[42] which can be related to density changes through the Lorentz−Lorenz equation. Dilatometry and refractometry allow characterization of the extent of physical aging in the nonequilibrium glass without altering the thermodynamic state of the specimen. As indicated above, physical aging is a consequence of the nonequilibrium glassy state; therefore, it is reversible upon heating the glass to temperatures above its T_g (equilibrium liquid state) followed by rapid quenching to the glassy state. As the nonequilibrium glass is heated above its glass transition, the reduction or loss in enthalpy that occurred in the glassy state is recovered. In a calorimetric (DSC) scan, this recovery in enthalpy is evident as an endothermic peak in the vicinity of the glass−rubber transition.[43,44] In this investigation, we use the recovered enthalpy from a nonisothermal DSC scan to characterize physical aging in semicrystalline PPS. The recovered enthalpy was calculated as the integrated area of the endothermic peak (enthalpic overshoot) obtained by subtracting the DSC scan for the unaged specimen from that of the corresponding aged specimen of interest.

The wholly amorphous and the four semicrystalline PPS samples were aged at 15 ± 2 °C below their $T_{g-onset}$ for 5, 24, and 168 h. Figure 2 shows the recovered enthalpy (ΔH) for the physically aged, wholly amorphous PPS sample plotted as a function of aging time (t_a). The recovered enthalpy increases systematically with increasing aging time, indicating that the nonequilibrium glass is closer to equilibrium at longer aging times. The data suggest a linear relationship between recovered enthalpy and log(t_a); this allows us to estimate the enthalpy relaxation rate (β_H), which is a reasonable indicator of the kinetics of physical aging:[45]

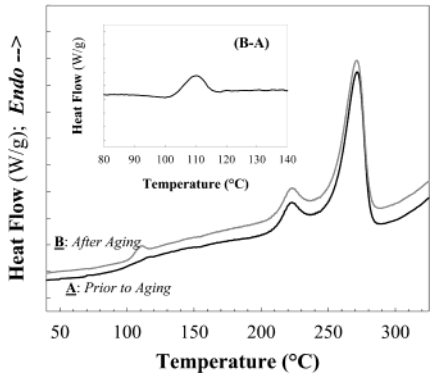

Figure 3. DSC traces of a representative semicrystalline PPS sample crystallized at 195 °C prior to and after aging at [$T_{g-onset}$ − 15] °C for 24 h. The inset shows the endothermic overshoot peak representative of the enthalpic recovery for the aging condition indicated.

$$\beta_H = \frac{d[\Delta H]}{d[\log (t_a)]} \tag{3}$$

It is important to note that while the enthalpy relaxation rate is a reasonable indicator of physical aging rate, it is not easily related to other measures of aging kinetics such as volume recovery rate and creep recovery rate. From Figure 2, we estimate β_H for wholly amorphous PPS to be equal to 1.46 J/(g decade) for the aging temperature chosen.

Our primary interest in this investigation, as outlined earlier, is to characterize physical aging in semicrystalline PPS. In Figure 3, DSC scans for a representative semicrystalline PPS sample prior to and after physical aging for 24 h are shown. The glass transition for the semicrystalline sample is characterized by a step change in heat capacity. For the physically aged specimen, an endothermic overshoot across the glass transition is clearly evident. The inset in Figure 3 shows the DSC scan for the semicrystalline specimen subtracted from that of the physically aged sample; this reveals the endothermic peak that is representative of the enthalpic relaxation process. It is clear that the enthalpic relaxation of the nonequilibrium semicrystalline glass is significant and easily quantifiable. The enthalpic relaxation endotherms in the semicrystalline PPS samples are observed to span a broad temperature range relative to their wholly amorphous counterpart.

The aging process did not change the characteristics [T_{m-1}, T_{m-2}, and $(\Delta H)_m$] of the melting endotherms for all the semicrystalline specimens. Further, the aging history did not alter the $\Delta C_p(T_g)$ for the semicrystalline specimens. Consequently, the relative fractions of the mobile-amorphous phase, the rigid-amorphous phase, and the crystalline phase remain unchanged after the aging treatment. This is consistent with Struik's model, as our aging experiments are performed well below the observed glass−rubber transition of the semicrystalline specimens (region 1 in Struik's model).

In Figure 4, the recovered enthalpy for the semicrystalline PPS specimens is plotted as a function of log(t_a). As expected, one notes a systematic increase in recovered enthalpy with increasing aging time for all of the semicrystalline specimens. Further, the recovered enthalpies of the semicrystalline samples are observed to be substantially lower than that of the wholly amorphous specimen. This observation of reduced aging in semicrystalline PPS is consistent with those of Tant and

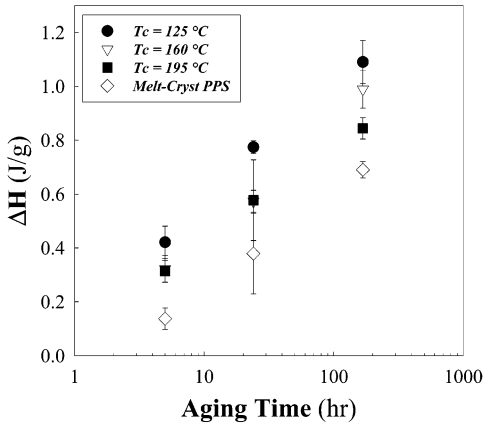

Figure 4. Recovered enthalpy (ΔH) plotted as a function of aging time for the four semicrystalline PPS samples investigated. The aging was carried out at [$T_{g-onset}$ − 15] °C.

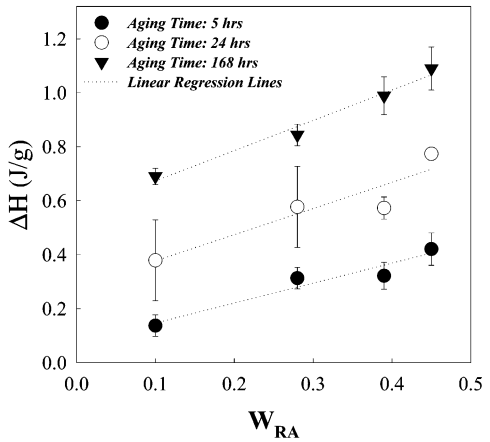

Figure 5. Recovered enthalpy (ΔH) plotted as a function of rigid-amorphous phase fraction and aging time for the four semicrystalline PPS samples investigated. The aging was carried out at [$T_{g-onset}$ − 15] °C.

Wilkes,[27] who report a linear dependence of aging rates on percent crystallinity in PET for crystallinities above 20%. While Tant and Wilkes demonstrate slower aging kinetics with increasing crystallinity, the relative influence exerted by the mobile-amorphous and rigid-amorphous phases on the physical aging characteristics in semicrystalline polymers could not have been addressed at the time as the concept of the rigid-amorphous phase was introduced subsequently.[35,36] In Figure 4, for each aging history, we observe that the recovered enthalpy is dependent on the semicrystalline morphology. This implies that a relationship between the physical aging kinetics and the relative proportions of the mobile-amorphous and the rigid-amorphous phases exists for semicrystalline PPS.

In Figure 5, the recovered enthalpy for each aging history is plotted as a function of the rigid-amorphous phase fraction in the corresponding PPS sample. For each aging history, we observe a systematic increase in the recovered enthalpy with increasing amounts of the rigid-amorphous phase fraction. This dependence on rigid-amorphous phase fraction is noted to be stronger at longer aging times. The extent of physical aging, characterized by the recovered enthalpy, is greater for specimens with a higher rigid-amorphous phase fraction.

The linear dependence of recovered enthalpy on log(t_a) allows us to calculate the enthalpic relaxation rate,

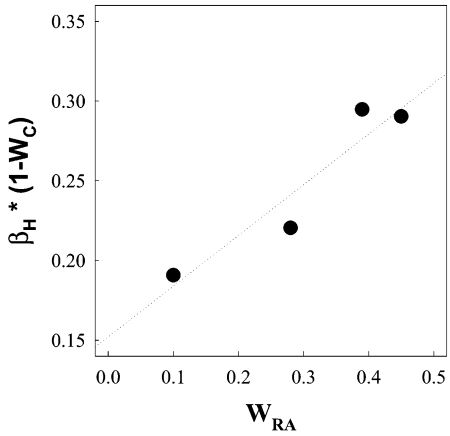

Figure 6. Normalized enthalpic relaxation rate plotted as a function of rigid-amorphous phase fraction for the four semicrystalline PPS samples investigated. The aging was carried out at [$T_{g-onset}$ − 15] °C.

β_H, for all the semicrystalline PPS samples investigated. In Figure 6, the enthalpic relaxation rate normalized with respect to the noncrystalline phase fraction [β_H*(1 − W_C)] is plotted as a function of the rigid-amorphous phase fraction. Such a normalization is justified as the crystalline phase is immune to physical aging. Here, we observe that the enthalpic relaxation rate is dependent on the rigid-amorphous phase fraction, with higher rigid-amorphous phase fractions favoring accelerated aging rates. This is an unexpected trend, considering that the rigid-amorphous phase is expected to possess a higher T_g compared to that of the mobile-amorphous phase. It is, perhaps, due to this counterintuitive observation that an extrapolation of the trend in Figure 6 to $W_{RA} = 0$ does not yield a β_H that is similar in magnitude to the corresponding value for wholly amorphous PPS.

Discussion

While enthalpy relaxation from nonisothermal DSC sweeps has been used to characterize aging in amorphous polymers, aged nylon[32] and aged semicrystalline PEEK[46] specimens did not show the endothermic peak across their glass−rubber transition. However, we have been able to characterize aging in semicrystalline PPS using enthalpy relaxation as a measure of the extent of densification. The endothermic overshoots, as depicted in Figure 3, have been quite amenable to integration such that a measure of recovered enthalpy can be extracted. This is perhaps due to the relatively high molecular weight of the PPS we are working with, which leads to a lower degree of overall crystallinity for a given crystallization history.

From the results presented above, it is clear that physical aging can be significant in relatively low-crystallinity polymers such as PPS. Therefore, this aspect must be considered when semicrystalline PPS (and other polymers) is designed for use in applications that involve prolonged exposure to temperatures close to their T_g. Physical aging can have particularly profound implications in applications that call for long service times in addition to mechanical and chemical stability because aging is known to substantially shorten failure times in creep rupture, fatigue, and stress cracking tests.[47]

In our investigations, the semicrystalline PPS samples were aged at 15 °C below their T_g. This corresponds to

region 1 in Struik's model,[28] wherein both the rigid- and mobile-amorphous phases undergo physical aging. Our observations indicate that the physical aging process is strongly dependent on the details of the semicrystalline morphology and not merely on the weight fraction of the crystalline phase. Specifically, we have observed that the rigid-amorphous phase helps accelerate the physical aging process compared to the mobile-amorphous phase in semicrystalline PPS. This is a new revelation and is counterintuitive considering that the rigid-amorphous phase is thought to possess a higher T_g compared to that of the mobile-amorphous phase. Let us consider this discovery in terms of the sub-glass relaxations in a similar polymer. Semicrystalline PEEK is known to display two distinct sub-glass relaxations; the low-temperature one is referred to as the β_1 relaxation, and the high-temperature one is referred to as the β_2 relaxation.[21,48−51] Specifically, based on dynamic mechanical data at 1 Hz, the β_1 relaxation peak is located at approximately −68 °C, while the β_2 relaxation peak is located at approximately −27 °C.[21] The β_1 relaxation is thought to correspond to highly localized, noncooperative motions in the bulk of the amorphous regions, and the β_2 relaxation is thought to correspond to cooperative motions in relatively organized regions of the noncrystalline phase.[21] In other words, the β_1 relaxation originates primarily from the mobile-amorphous phase, while the β_2 relaxation originates primarily from the rigid-amorphous phase. It is important to note that the β_2 relaxation is of a cooperative nature with a substantially higher activation energy compared to the β_1 relaxation. Therefore, it is possible that the cooperative segmental motions that originate from the rigid-amorphous phase help accelerate the physical aging process in semicrystalline PPS. After all, localized segmental motions do facilitate the thermodynamic changes that occur during the aging process. While we have drawn on the sub-glass relaxations in semicrystalline PEEK to explain our observations concerning the influence of the rigid-amorphous phase on the physical aging process, we will need to confirm the same for PPS. This work is in progress and will be reported on in the near future.

Shelby and Wilkes[52,53] reported that the physical aging kinetics, as deciphered through volume relaxation, in oriented polystyrene and polycarbonate was considerably accelerated compared to that of their isotropic counterparts despite the fact that the overall free volume is lower in the oriented specimens. They suggest that the oriented state serves to overcome certain activation barriers (such as bond rotation and molecular rearrangement) such that the configurational changes that lead to a denser packing of the chains occur more rapidly; this, of course, increases the volume relaxation rate. The above hypothesis was supported by dynamic mechanical characterization of the oriented and isotropic specimens with the oriented samples displaying stronger sub-glass β relaxations. This analysis allows us to hypothesize that the rigid-amorphous phase, which includes chain segments that are more tightly packed relative to the mobile-amorphous phase, is able to increase the enthalpic relaxation rates due to its relative proximity to a state of even lower configurational entropy. Perhaps, localized segmental relaxations within the rigid-amorphous phase also assist this time-dependent process of physical aging.

In our aging experiments (Struik: region 1), we expect both the rigid- and mobile-amorphous phases to experience the consequences of physical aging. Struik's model[28] states that the extent of aging should be greater in the mobile-amorphous phase relative to the rigid-amorphous phase in region 1, based solely on the proximity of the aging temperature to the glass transition temperature of the two phases. However, our observations on semicrystalline PPS suggest that the configurational entropic state of the mobile- and the rigid-amorphous phases are perhaps more relevant to physical aging than the proximity of the aging temperature to their respective glass transition temperatures.

While the previous paragraphs outline possible explanations for the observed relationship between the rigid-amorphous phase fraction and physical aging rates, we now attempt to offer workable solutions to minimize the consequences of aging in semicrystalline PPS applications. One obvious approach is to impose a process history that minimizes the rigid-amorphous phase fraction in the PPS part; melt-crystallization via slow cooling and cold-crystallization at high temperatures will accomplish this. Alternately, PPS copolymers with small amounts (<10%) of *meta*-connected phenylene moieties (accomplished through a combination of 1,3-dichlorobenzene and 1,4-dichlorobenzene) crystallize slower and to a lesser extent compared to the all-*para* homopolymer. Further, at similar crystallization conditions, PPS copolymers with the *meta*-connected phenylene moieties display substantially lower rigid-amorphous phase fractions compared to the all-*para* homopolymer.[16,17] Similar results were observed with poly(ether ketone ketone) copolymers as well.[22] Therefore, PPS copolymers with small amounts of the *meta*-connected phenylene moieties may be better candidates for applications that call for extended exposure to relatively high temperatures. However, such copolymers will also tend to be less crystalline for a given crystallization history. Finally, for a given end-use temperature, increasing the T_g of the PPS via blending with an appropriate high-T_g amorphous polymer that is at least partially miscible with PPS can slow the physical aging rates as well.

While our aging experiments were carried out at a fixed distance from the T_g of the mobile-amorphous phase (T_g^L), this aging temperature is likely to be at varying separation from the T_g of the rigid-amorphous phase (T_g^U). Consequently, our aging condition may not be consistent for the different PPS samples. Further, we use enthalpy relaxation as our only measure of the extent of aging. This is characterized by integrating the endothermic peak across the T_g of the mobile-amorphous phase. Does this mean that we are only quantifying the extent of aging that occurred in the mobile-amorphous phase, while we have every reason to believe that aging occurred in the rigid-amorphous phase as well? Does the breadth of the enthalpic relaxation peak suggest that it contains contributions from both the rigid- and mobile-amorphous phases? Finally, if we are only characterizing aging in the mobile-amorphous phase, does the fact that the aging kinetics are faster in samples with a higher rigid-amorphous phase fraction suggest that this rigid phase is somehow promoting the aging process in the mobile-amorphous phase? Obviously, we have several questions that are yet to be answered, and we hope to address at least some of them

in subsequent studies. One experimental technique that may help address some of the above-mentioned issues is temperature-modulated DSC (TM-DSC). This technique may be able to decouple T_g^L and T_g^U from any melting endotherms such that one may be able to conduct aging experiments at temperatures that are equidistant from both T_g^U and T_g^L.

Conclusions

In this work, we have investigated the influence of semicrystalline morphology on the physical aging behavior of PPS. We characterize the semicrystalline morphology of PPS in terms of the three-phase model comprising of a mobile-amorphous phase, a rigid-amorphous phase, and a crystalline phase. Cold-crystallization of wholly amorphous specimens at various temperatures, and melt-crystallization provided us with specimens of widely differing morphologies. Cold-crystallization at higher temperatures and melt-crystallization resulted in relatively lower amounts of the rigid-amorphous phase. This is consistent with a lower degree of constraint imposed by the crystallites on the mobility of the noncrystalline chain segments when crystallization occurs under conditions of high segmental mobility.

The wholly amorphous and the semicrystalline PPS specimens were aged at approximately ($T_{g-onset}$ − 15) °C for 5, 24, and 168 h. The extent and kinetics of physical aging in these samples were characterized using enthalpic relaxation rates determined from nonisothermal DSC sweeps across the glass−rubber transition. The recovered enthalpy of all of the samples displayed the classical linear dependence on log(t_a). While the enthalpic relaxation rates of the semicrystalline specimens are substantially lower than that of their wholly amorphous counterpart, our experiments indicated that the extent of physical aging in semicrystalline PPS is significant and easily quantifiable. As a result, physical aging must be considered when semicrystalline PPS is designed for use in applications that involve prolonged exposure to above-ambient temperatures.

We have observed that the enthalpic relaxation rate in semicrystalline PPS is sensitive to the relative amounts of the rigid-amorphous and mobile-amorphous phases. Specifically, for a given aging history, the enthalpic relaxation rate was observed to increase with increasing amounts of the rigid-amorphous phase. This is a counterintuitive result if one considers the rigid-amorphous phase to possess a higher T_g compared to that of the mobile-amorphous phase. However, this new finding is consistent with previous research on molecular orientation facilitating accelerated aging in certain amorphous polymers.[52,53] Like with the oriented systems, it is possible that the relatively ordered rigid-amorphous phase requires lower activation to proceed to a state of even lower configurational entropy during the aging process. In other words, the rigid-amorphous phase, which includes chain segments that are more tightly packed relative to the mobile-amorphous phase, is perhaps able to increase the enthalpic relaxation rates due to its relative proximity to a state of lower configurational entropy. Further, prior dynamic mechanical characterization of semicrystalline PEEK, a polymer not unlike PPS in its crystallization behavior, revealed a cooperative sub-glass relaxation associated with the rigid-amorphous phase.[21] Therefore, it is also possible that such localized relaxations (that are of a cooperative nature) within the rigid-amorphous phase facilitate molecular rearrangements that accelerate the aging process.

The observations reported here also suggests that the configurational entropic state of the mobile-amorphous and the rigid-amorphous phases are perhaps more relevant to physical aging in semicrystalline polymers than the proximity of the aging temperature to their respective glass transition temperatures.

Acknowledgment. The encouragement and assistance offered by Prof. Garth Wilkes (Virginia Tech) and Prof. Stephen Cheng (University of Akron) are greatly appreciated. The authors also thank Prof. Greg McKenna (Texas Tech University) for useful comments and for pointing us to some relevant references. Dr. Paul DesLauriers and his group are acknowledged for molecular weight measurements on the subject polymer. Finally, Chevron Phillips Chemical Co. is acknowledged for encouragement and permission to publish this work.

References and Notes

(1) Geibel, J. F.; Leland, J. E. In *Kirk-Othmer Encyclopedia of Chemical Technology*; John Wiley and Sons: New York, 1996; Vol. 19, p 904.
(2) Geibel, J. F.; Campbell, R. W. In *Comprehensive Polymer Science;* Eastwood, G. C., et al., Eds.; Pergamon Press: Oxford 1990; Vol. 5.
(3) Hill, H. W.; Brady, D. G. In *Encyclopedia of Chemical Technology*, 3rd ed.; John Wiley and Sons: New York, 1982; Vol. 18, p 793.
(4) Lopez, L. C.; Wilkes, G. L. *J. Macromol. Sci.: Rev. Macromol. Chem. Phys.* **1989**, *C29*, 83.
(5) Lovinger, A. J.; Davis, D. D.; Padden, F. J. *Polymer* **1985**, *26*, 1595.
(6) Lopez, L. C.; Wilkes, G. L. *Polymer* **1988**, *29*, 106.
(7) Lopez, L. C.; Wilkes, G. L.; Geibel, J. F. *Polymer* **1989**, *30*, 147.
(8) Mehl, N. A.; Rebenfeld, L. *Polym. Eng. Sci.* **1992**, *32*, 1451.
(9) Cheng, S. Z. D.; Wu, Z. Q.; Wunderlich, B. *Macromolecules* **1987**, *20*, 2802.
(10) Chung, J. S.; Cebe, P. *Polymer* **1992**, *33*, 2312.
(11) Chung, J. S.; Cebe, P. *Polymer* **1992**, *33*, 2325.
(12) Chung, J. S.; Cebe, P. *J. Polym. Sci.: Polym. Phys. Ed.* **1992**, *30*, 163.
(13) Huo, P.; Cebe, P. *Colloid Polym. Sci.* **1992**, *270*, 840.
(14) Menczel, J. D.; Collins, G. L. *Polym. Eng. Sci.* **1992**, *32*, 1264.
(15) Collins, G. L.; Menczel, J. D. *Polym. Eng. Sci.* **1992**, *32*, 1270.
(16) Wu, S. S.; Kalika, D. S.; Lamonte, R. R.; Makhija, S. *J. Macromol. Sci.: Macromol. Phys. Ed.* **1996**, *B35*, 157.
(17) Kalika, D. S.; Wu, S. S.; Lamonte, R. R.; Makhija, S. *J. Macromol. Sci.: Macromol. Phys. Ed.* **1996**, *B35*, 179.
(18) Cheng, S. Z. D.; Cao, M. Y.; Wunderlich, B. *Macromolecules* **1986**, *19*, 1868.
(19) Huo, P.; Cebe, P. *Macromolecules* **1992**, *25*, 902.
(20) Kalika, D. S.; Krishnaswamy, R. K. *Macromolecules* **1993**, *26*, 4252.
(21) Krishnaswamy, R. K.; Kalika, D. S. *Polymer* **1994**, *35*, 1157.
(22) Krishnaswamy, R. K.; Kalika, D. S. *Polymer* **1996**, *37*, 1915.
(23) McKenna, G. B. In *Comprehensive Polymer Science;* Booth, C., Price, C., Eds.; Pergamon Press: Oxford, 1990; Vol. 2.
(24) Tant, M. R.; Wilkes, G. L. *Polym. Eng. Sci.* **1981**, *21*, 874.
(25) Struik, L. C. E. *Physical Aging in Amorphous Polymers and Other Materials*; Elsevier: New York, 1978.
(26) McKenna, G. B.; Simon, S. L. In *Polymers and Composites*; American Society for Testing and Materials: 2000.
(27) Tant, M. R.; Wilkes, G. L. *J. Appl. Polym. Sci.* **1981**, *26*, 2813.
(28) Struik, L. C. E. *Polymer* **1987**, *28*, 1521.
(29) Struik, L. C. E. *Polymer* **1987**, *28*, 1534.
(30) Struik, L. C. E. *Polymer* **1989**, *30*, 799.
(31) Struik, L. C. E. *Polymer* **1989**, *30*, 815.
(32) Spinu, I.; McKenna, G. B. *Polym. Eng. Sci.* **1994**, *34*, 1808.
(33) Beckmann, J.; McKenna, G. B.; Landes, B. G.; Bank, D. H.; Bubeck, R. A. *Polym. Eng. Sci.* **1997**, *37*, 1459.

(34) Spinu, I.; McKenna, G. B. *J. Plast. Film Sheeting* **1997**, *13*, 311.
(35) Suzuki, H.; Grebowicz, J.; Wunderlich, B. *Makromol. Chem.* **1985**, *186*, 1109.
(36) Suzuki, H.; Wunderlich, B. *Br. Polym. J.* **1985**, *17*, 1.
(37) Kumar, S. K.; Yoon, D. Y. *Macromolecules* **1989**, *22*, 4098.
(38) Kumar, S. K.; Yoon, D. Y. *Macromolecules* **1991**, *24*, 5414.
(39) Sauer, B. B.; Hsiao, B. S. *Polymer* **1995**, *36*, 2553.
(40) Verma, R.; Marand, H.; Hsiao, B. S. *Macromolecules* **1996**, *29*, 7767.
(41) Greiner, R.; Schwarzl, F. R. *Rheol. Acta* **1984**, *23*, 378.
(42) Robertson, C. G.; Wilkes, G. L. *Polymer* **1998**, *39*, 2129.
(43) Petrie, S. E. B. *J. Polym. Sci., Part A-2* **1972**, *10*, 1255.
(44) Hutchinson, J. M. *Prog. Colloid Polym. Sci.* **1992**, *87*, 69.
(45) Hutchinson, J. M. *Prog. Polym. Sci.* **1995**, *20*, 703.
(46) Ogale, A. A. Elastic and Viscoelastic Properties of Advanced Thermoplastics and Their Short-Fiber Composites, Report Number CCM87-20, Center for Composite Materials, University of Delaware, Dec 1986.
(47) Arnold, J. C. *Polym. Eng. Sci.* **1995**, *35*, 165.
(48) David, L.; Etienne, S. *Macromolecules* **1992**, *25*, 4302.
(49) Sasuga, T.; Hagiwara, M. *Polymer* **1985**, *26*, 501.
(50) Sasuga, T.; Hagiwara, M. *Polymer* **1986**, *27*, 821.
(51) Sasuga, T.; Hagiwara, M. *Polymer* **1987**, *28*, 1915.
(52) Shelby, M. D.; Wilkes, G. L. *Polymer* **1998**, *39*, 6767.
(53) Shelby, M. D.; Wilkes, G. L. *J. Polym. Sci., Polym. Phys. Ed.* **1998**, *36*, 2111.

MA025776U